Graphene stripper foils

Igor Pavlovsky[a] and Richard L. Fink
Applied Nanotech, Inc., 3006 Longhorn Blvd., Suite 107, Austin, Texas 78758

(Received 3 January 2012; accepted 23 February 2012; published 20 March 2012)

Thin carbon and metal foils have been used in heavy ion accelerators for charge stripping. The power dissipated by a particle beam in a foil can be as high as 3 kW or greater, which results in short lifetimes of conventional stripper foils. Graphene stripper foils can overcome critical limitations of other materials due to a unique combination of their exceptional physical properties. The authors have fabricated graphene foils with diameters up to 13 cm and area densities of 0.1 to 3.0 mg/cm^2 by reduction of graphene oxide in an aqueous dispersion followed by pressure filtration. The foils were characterized by a number of analytical techniques, including scanning electron microscopy, thermogravimetric analysis, and x-ray photoelectron spectroscopy, and proved their superior mechanical and thermal properties. Preliminary ion beam tests showed that the graphene stripper foils possess up to four times longer lifetime, as opposed to conventional carbon foils. © *2012 American Vacuum Society*. [http://dx.doi.org/10.1116/1.3693594]

I. INTRODUCTION

The remarkable physical properties of graphene have triggered considerable interest to this material in the last several years. Due to its high thermal conductivity, high surface area, unique electronic and mechanical properties, graphene can find potential use in electronic devices,[1,2] composite materials,[3] field emission devices,[4] sensors,[5] ultracapacitors,[6] optical devices,[7] and many other applications. Graphene can be of special interest to the nuclear physics community as it has a number of physical properties which are critical for demanding charge stripper foil applications.

A stripper foil is a crucial element of a heavy ion accelerator. Introduction of stripper foils in an accelerator easily increases the variety of ion acceleration techniques available and therefore decreases the accelerator construction cost. By way of example, the RIKEN RI-beam facility in Japan is designed to strip a beam of uranium 72 + at 50.5 MeV/nucleon to 88 + ion state by a 14 mg/cm^2 thick carbon stripper foil. The power dissipated by the beam in the foil is about 3 kW.[8] This power can easily damage a carbon foil placed in a vacuum chamber. To handle such high power loads over a small beam size (about 1–2 mm diameter), the design of the stripper foil includes rotating the foil during beam irradiation to enlarge the area of thermal loading and radiative cooling of the foil.

Standard stripper foil materials are amorphous or glassy carbon. These foils are typically expensive to make, fragile and difficult to make over a large area. Amorphous carbon also has poor thermal and electrical conductivity; the poor heat transfer leads to greater susceptibility of evaporation and damage from local beam heating. Moreover, the foil should be thin enough to avoid unnecessary beam attenuation, and thick enough to provide efficient charge stripping.

There is a need for a stripper foil that is thermally conductive (significantly better than amorphous carbon), made of low-Z material, and mechanically robust such that it can be handled and mounted on a mandrel for rotation at high angular frequencies. The rotating foil should be highly uniform so that the beam energy oscillations are less than or at least comparable to the ion energy straggling, which is typically less than 0.1%.[8] The foil should be robust against heavy ion radiation damage, and should be fabricated to large areas at low cost. Properly fabricated graphene stripper foils, as described below, can potentially meet all these requirements.

II. MODELING

In order to prepare a proper stripper foil, one must know what is needed and how the foil will be used in order to achieve the desired results. We have performed modeling calculations of temperature distributions of a rotating stripper foil using the parameters of our fabricated graphene foils and the operating conditions expected under ion beam irradiation. We used COMSOL MULTIPHYSICS 3.5a modeling and simulation software which is capable of performing finite element analysis of thermal and other physical properties of materials.

In our calculations, we considered a Gaussian beam with a radius of 0.25 cm and 200 W dissipated beam power. The foil diameter was 13 cm, the diameter of the beam trajectory circle was 11.5 cm, and the diameter of the mandrel was 10 cm. The modeled foil thickness was 3 μm, which is equivalent to the foil area density of 0.53 mg/cm^2 provided that the graphene film has a bulk density of approximately 1.8 g/cm^3. The anisotropic temperature dependent thermal conductivity values were defined as $k_x = k_y = (38 + 346\,000/(T - 60))$ and $k_z = (0.3 + 760/(T - 110))$, where the temperature T is in K. The temperature dependence of the specific heat capacity was defined as $C_p = (12.7 + 2.872T - 0.00145T^2 + 3.12 \times 10^{-7}T^3 - 2.38 \cdot 10^{-11}T^4)$. The heat equation accounted for both the heat transfer via heat conduction to the foil mandrel and the radiation losses from both sides of the foil. We used the graphene emissivity value of 0.8 and the ambient temperature of 273 K.

The results of the modeling of a stationary foil are shown in false colors in Fig. 1. The maximum temperature that was

[a]Electronic mail: ipavlovsky@appliednanotech.net

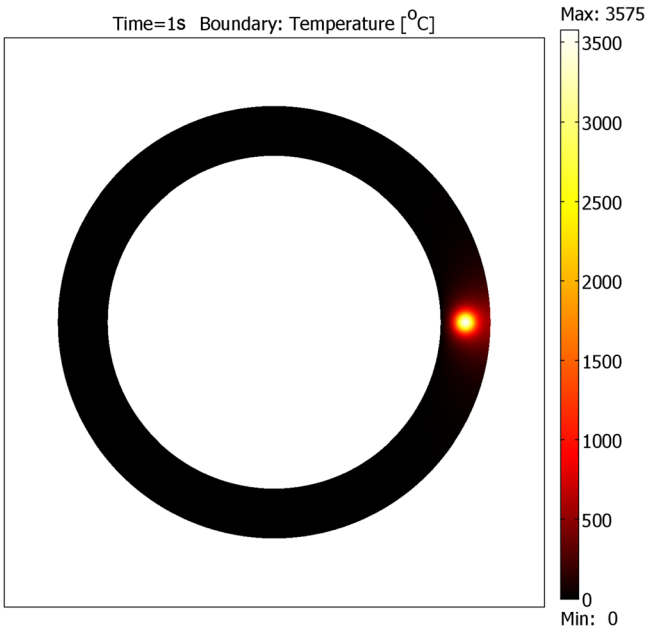

FIG. 1. (Color online) Temperature distribution calculation of a stationary graphene foil.

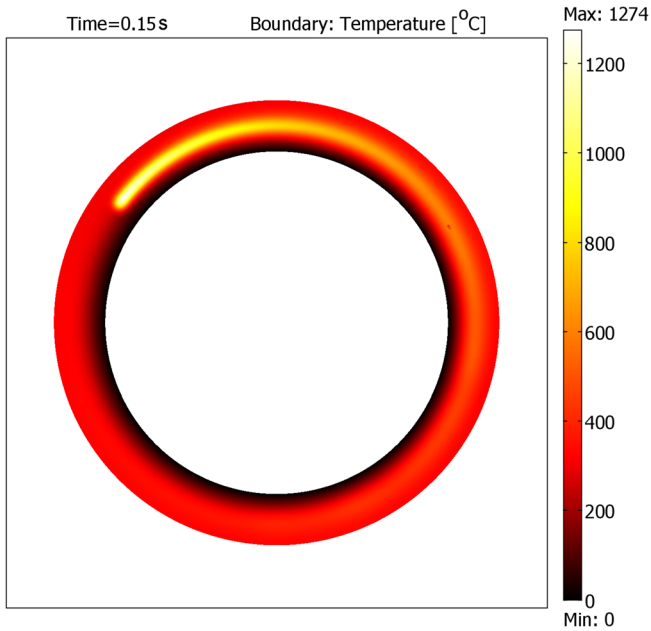

FIG. 2. (Color online) Temperature distribution calculation of a graphene foil rotating at an angular frequency of 100 rad/s after 0.15 s.

reached in the center of the ion beam spot was found to be 3575 °C, which is just below the sublimation point for graphite. However, practical values of the maximum temperature for carbon stripper foils are usually below approximately 2000 °C, otherwise the foil stability and lifetime drastically decreases.

The results of the modeling of a graphene stripper foil rotating at a 100 rad/s angular frequency is shown in Fig. 2. The boundary temperature plot shows that the dissipated heat spreads much more evenly over the entire foil area, resulting in significant lowering of the maximum foil temperature. In this case, the calculated maximum temperature in the center of the ion beam spot is 1274 °C. The maximum temperature reaches the equilibrium value after approximately 2 s. The modeled foil shown in Fig. 2 simulated clockwise rotation. For modeling purposes, the beam spot was rotated and the foil fixed. This causes the hot spot to appear on the left side in Fig. 2.

A number of physical parameters were varied in the model in order to establish the most appropriate routes for optimization of both the foil properties and operating conditions. We found that a possible increase in either graphene emissivity or thermal conductivity would result only in a marginal decrease in the maximum foil temperature, typically within 100 °C. The calculations show that poor thermal conductivity of the graphene in the direction of c axis does not significantly affect the maximum foil temperature. Indeed, the heat transfer to the mandrel is not very significant as the foil is very thin; therefore radiation losses appear to be the key mechanism for foil cooling. Also, calculations show that higher angular frequencies can considerably decrease the temperature of the rotating foil. Thus, increasing the angular frequency of rotating stripper foils can be one of the most appropriate ways to lower foil temperature under the beam irradiation. It is noteworthy that the rotating foil temperature can also be significantly lower for a material with higher heat capacity, C_p. Though the heat capacity can hardly be tailored for graphene, the actual temperature dependence of C_p appears to be very favorable, as it increases significantly with temperature. Proper definition of $C_p(T)$ provides a much smoother temperature profile as opposed to the profile calculated using a constant C_p.

The results of the modeling show that a rotating graphene foil can allow much higher beam loads and significantly increased foil lifetimes due to a distributed and thus considerably weakened radiation damage. The feasibility of making of such graphene foils and characterization of their physical properties is discussed below.

III. EXPERIMENT

We prepared graphene foils using a method previously described by Chen *et al.*[9] The method is based on a controlled reduction of graphene oxide by hydrazine with addition of ammonia in an aqueous dispersion. The dispersion of graphene oxide with loading of 0.5 wt. % in water was obtained from Angstron Materials. The dispersion was reduced for 4 h at 95 °C and then cooled down to room temperature. The thickness of graphene foils was controlled by using a calculated volume of graphene dispersion knowing the loading of graphene. A commercially available stainless steel filter holder was used to make graphene foils by pressure filtration. The diameter of the fabricated foils was 13 cm. The filter holder allowed increasing the differential pressure across the filter. A compressed air line with a pressure regulator was connected to the filter holder to pressurize the air space above the graphene dispersion. Pressure up to 300 kPa was used to filter the dispersion. Commercially

FIG. 3. Photograph of a free-standing graphene foil.

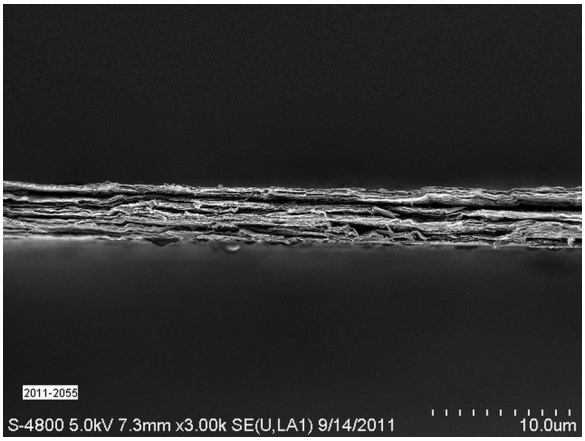

FIG. 4. SEM of a cross-section of a free-standing graphene foil.

available polymer filter membranes with a diameter of 142 mm were used for the filtration.

After filtration, graphene foils still on the filter membrane were removed from the filter holder and peeled off the filter membrane to obtain free-standing graphene foils. Dried graphene foils display a shiny metallic luster on both sides. Figure 3 shows a photograph of a free-standing foil with an area density of 0.5 mg/cm^2 (the foil thickness is approximately 3 μm) and a diameter of 13 cm. The described fabrication method allowed us to consistently obtain complete, undamaged, pinhole free graphene foils. The graphene foils can then be easily cut into samples of a required size, handled by hand and weighed using a micro-balance to calculate the area density.

After drying, the foils were typically cut into samples of a smaller size, typically 4–5 cm rectangles, and baked in a tube furnace in air or forming gas (4% H_2 in N_2). Baking of graphene foils in air at temperatures of 450 °C and above resulted in full decomposition (oxidation to CO_2) of the films within less than one hour. Lower baking temperatures resulted in a partial loss of foil mass. Baking of foils in forming gas or nitrogen at high temperatures resulted in a 20–30 % mass loss. The foil characterization discussed below was performed for as-prepared and baked foils.

IV. RESULTS AND DISCUSSION

Scanning electron microscopy (SEM) of graphene foils was performed using a Hitachi S-4800 microscope. The image in Fig. 4 shows a cross-sectional view of a 0.55 mg/cm^2 foil. Based on the area and mass of the foil sample, we estimate that the foil density is approximately 1.8 g/cm^3, which is comparable to the density of bulk graphite being 2.2 g/cm^3. This result indicates that the graphene crystallites are tightly packed in the foil.

We measured the area mass density of the fabricated foils by measuring sample area and weight using a microbalance. The measured foil density was in the range of 0.1 to 3.1 mg/cm^2, that corresponds to the foil thickness of approximately 0.6 μm to over 17 μm. In addition to the area density measurements, we measured the sheet resistance of the foils. The plot for sheet conductivity versus area density of the foils is shown in Fig. 5. The results demonstrate good consistency in foil fabrication. Based on this nearly linear dependence, we can calculate an average value for bulk resistivity of the foils, which equals approximately 1.9×10^{-2} Ohm cm. This value is significantly lower than the reported value for in-plane bulk resistivity of HOPG grade graphite ($3.5 - 4.5 \times 10^{-5}$ Ohm cm[10]). This indicates that there is a significant contact resistance between the individual graphene crystallites that make up the film, which is most likely due to both the intercrystallite boundaries and nonreduced oxygen: heat-treatment of graphene paper was reported[9] to increase its conductivity due to thermal deoxygenation.

As stated above, the foil mass decreases by 20–30 % after baking. We performed a thermogravimetric analysis (TGA) of the films in order to establish the nature of the mass loss. TGA was conducted using a Q50 analyzer. The foils were analyzed in nitrogen atmosphere using a temperature ramp to 800 °C. Three desorption peaks were found: near 50, 200, and 600 °C (see Fig. 6). We speculate that the first peak may be due to the release of entrapped water. The second peak

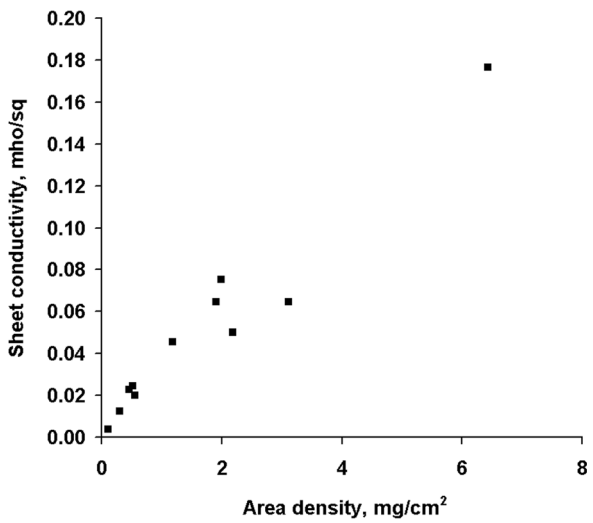

FIG. 5. Dependence of sheet conductivity on area density of graphene foils.

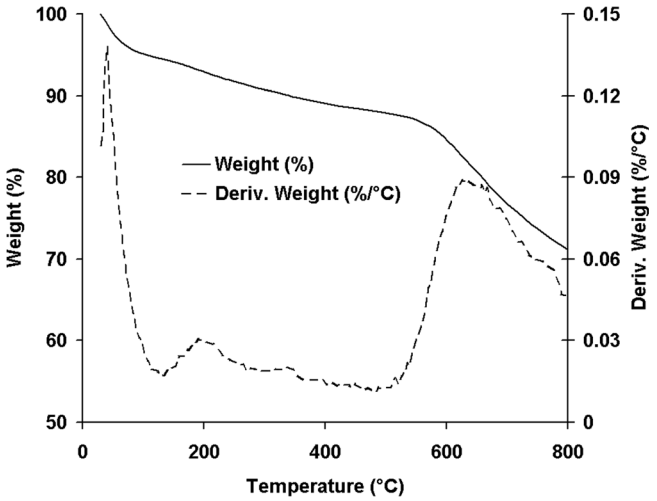

FIG. 6. TGA analysis of a graphene foil sample.

was most likely due to desorption of oxygen-containing groups,[11] and the third peak may be due to etching of amorphous carbon or the edges of graphene crystallites, and partly due to carbon oxidation to CO_2 by residual air.

X-ray photoelectron spectroscopy (XPS) analysis of graphene foils was performed in order to determine the content of graphene crystallites before and after baking in nitrogen and in forming gas. The Al Ka line beam spot size was 100 μm, the penetration depth was 3 nm, which was greater than the thickness of a single graphene crystallite. Thus we can assume that the XPS analysis was made effectively for the bulk material of the foil, not only for the foil surface. The results provided in Table 1 show that baking in forming gas resulted in the formation of graphene foils with the least content of nitrogen and also reduced oxygen content. On the other hand, baking in pure nitrogen almost did not change the chemical composition of the foils.

Measurements of the thermal conductivity of a thick graphene foil sample have been made using ASTM E1461 laser flash method by NETZSCH Instruments North America LLC. The following parameters were used for the calculation of the thermal conductivity: bulk density of the graphene foil sample 1.55 g/cm^3, temperature 25 °C and specific heat C_p 0.73 J/gK. The measured thermal diffusivity was 1308 mm^2/s. The thermal conductivity of the sample was found to be 1480 W/mK. High thermal conductivity of the graphene foils together with poor electrical conductivity points to a phonon dominated heat transfer mechanism in this material. The high thermal conductivity of the graphene foils such as the one found for the measured sample, can facilitate more efficient heat transfer across the entire foil area.

Samples of graphene foils were tested for tensile strength using a standard pull test. The average sample size was approximately 2 cm × 2 cm and the measured tension force was on the order of 10 N. Based on the dimensions of the foil samples and the values of the tension force, we have calculated the ultimate tensile strength (TS) of the samples. For as-prepared foils the TS was 167 ± 16 MPa, and for the foils baked at 600 °C the tensile strength was 74 ± 49 MPa. These

TABLE 1. XPS elemental analysis of baked and as-prepared graphene foils.

Foil	As-prepared	Baked in N_2 @600 °C	Baked in forming gas @600 °C
C content	89.6%	90.2%	96.1%
O content	8.8%	8.5%	3.9%
N content	1.6%	1.2%	0%

measurements show that baking of graphene foils at high temperatures, over 500 °C, resulted not only in a decrease in the tensile strength and poor consistency of the measured data, but, as mentioned above, in a significant mass loss. This indicates that during the heat treatment, uncontrollable internal defects can be formed in the foils. These findings are also consistent with results reported by Chen.[9]

We can use the measured values of the tensile strength for estimating the ultimate angular frequency of a rotating foil using the following equation:

$$\mathrm{TS} = \rho\omega^2(3+\nu/8)(R^2 - r^2), \quad (1)$$

where υ is the Poisson ratio, R is the radius of the foil disk, r is the radius of the foil holder (mandrel), and ρ is the bulk density of the foil. Using the parameters typical for our graphene foils, that is $\upsilon = 0.17$, $\rho = 1.8$ g/cm^3, $R = 6.5$ cm, $r = 5$ cm, and TS being 165 MPa, we can obtain that $\omega > 30\,000$ rad/s for the foil installed on the mandrel, and $\omega > 7000$ rad/s for the foil with a very small shaft radius ($r \to 0$). The angular frequency of 30 000 rad/s is two orders of magnitude greater than the targeted foil rotation frequency of 300 rad/s. Based on the provided calculations, both as-prepared and baked foils will survive rotation on a mandrel at the targeted angular frequency.

Preliminary tests of graphene foil targets under ion beam irradiation were performed at Michigan State University by Dr. Felix Marti. The tests were done under stationary target conditions as a spinning target facility is not available at this time. The tests were supported by the National Superconducting Cyclotron Laboratory (NSCL) development program at MSU.

The beam being stripped was ^{87}Kr ions at an energy of 13.0 MeV per nucleon. The foil lifetime was a key characterization parameter in these tests. Along with the graphene foils, amorphous carbon foils were used for beam stripping under the same test conditions. The foil lifetime was rated in terms of a percentage of the predicted lifetime (approximately 50 h in this test). A set of 20 amorphous carbon foils was tested in a single load of the stripper system. The measured lifetime of the amorphous carbon foils was found to be 70.0% ± 34.3%.

Two types of graphene foils were tested: as-prepared foils with an area density of 0.55 mg/cm^2 and treated in forming gas with an area density of 0.46 mg/cm^2. All of the tested foil samples were parts of a single large foil. Five foil samples were tested to determine their lifetimes. It was found that two of the five samples considerably exceeded the calculated lifetime during the tests: an as-prepared sample lasted 400% of the expected lifetime, while the lifetime of a

heat-treated sample was over 250% though the experiment was stopped due to a planned reloading of the stripper system. Three other foils, however, failed in this test. The reason for the failure was that the attachment procedure used for these graphene foils was different from the procedure developed for amorphous carbon foils. We are in the process of redesigning the foil holders to use a pocket structure to support the foils. More experimental statistics are needed to determine if treated or as-prepared foils have longer lifetimes and what changes may be needed to the foil installation procedures.

V. CONCLUSIONS

We have fabricated free-standing graphene foils with diameters of up to 13 cm by the controlled reduction of graphene oxide with hydrazine and ammonia in an aqueous dispersion followed by pressure filtration. The foil thickness was in the range of 0.6 to nearly 20 μm and the bulk density was approximately 1.8 g/cm^3. Peeled-off and dried foils exhibited metallic luster and were easy to handle. Characterization studies revealed high thermal conductivity and high tensile strength of the foils. Modeling of a rotating foil with physical properties as those found for the fabricated foils has shown that the foils can be good candidates for rotating stripper foil applications. Preliminary ion beam tests indicated that the foil samples exhibit very long lifetimes—by a factor of 4 longer than the lifetime expected for conventional carbon foils. These results indicate that graphene foils can find applications as windows for cells with gas targets.

ACKNOWLEDGMENTS

The authors would like to thank Felix Marti and the NSCL staff for performing characterization of graphene foil samples under ion beam irradiation. This material is based upon work supported by the Department of Energy under Award Number DE-SC0000852.

[1]Y. M. Lin, C. Dimitrakopoulos, K. A. Jenkins, D. B. Farmer, H. Y. Chiu, A. Grill, and P. Avouris, Science **327**, 662 (2010).
[2]F. Traversi, V. Russo, and R. Sordan, Appl. Phys. Lett. **94**, 223312 (2009).
[3]S. Stankovich, D. A. Dikin, G. H. B. Dommett, K. M. Kohlhaas, E. J. Zimney, E. A. Stach, R. D. Piner, S. B. T. Nguyen, and R. S. Ruoff, Nature (London) **442**, 282 (2006).
[4]I. Pavlovsky, U.S. Patent No. 6,819, 034 (21 August 2000)
[5]F. Schedin, A. K. Geim, S. V. Morozov, E. W. Hill, P. Blake, M. I. Katsnelson, and K. S. Novoselov, Nat. Mater. **6**, 652 (2007).
[6]M. D. Stoller, S. Park, Y. Zhu, J. An, and R. S. Ruoff, Nano Lett. **8**, 3498 (2008).
[7]H. Zhang, D. Tang, R. J. Knize, L. Zhao, Q. Bao, and K. P. Loh, Appl. Phys. Lett. **96**, 111112 (2010).
[8]H. Ryuto, S. Yokouchi, N. Fukunishi, H. Hasebe, N. Inabe, A. Goto, M. Kase, and Y. Yano, "Rotating Carbon Disk Stripper for Intense Heavy-Ion Beams," in *Proceedings of the 17th International Conference on Cyclotrons and Their Applications*, 18–22 2004, Particle Accelerator Society of Japan, Tokyo, Japan (2005).
[9]H. Chen, M. B. Müller, K. J. Gilmore, G. G. Wallace, and D. Li, Adv. Mater. **20**, 3557 (2008)
[10]See: http://www.tectra.de/hopg.htm
[11]S. Park, J. An, I. Jung, R. D. Piner, S. J. An, X. Li, A. Velamakanni, and R. S. Ruoff, Nano Lett. **9**, 1593 (2009).